EPR study of hole trapping at cation vacancies in silver halides

Chien-teh Kao, L. G. Rowan, and L. M. Slifkin
Department of Physics and Astronomy, University of North Carolina at Chapel Hill, Campus Box 3255, Phillips Hall, Chapel Hill, North Carolina 27599-3255
(Received 2 November 1989; revised manuscript received 12 March 1990)

Hole trapping at cation vacancies in doped, irradiated silver halides is studied by means of electron paramagnetic resonance (EPR). From detailed studies of the behavior of the EPR spectra upon thermal annealing and of the effects of the concentrations of various divalent cations, it is demonstrated that in AgCl the positive hole can indeed be bound to the negative cation vacancy. The resulting two types of paramagnetic centers, which survive up to 70 and 110 K, respectively, are identified as perturbed self-trapped hole centers with a cation vacancy in either the next-nearest-neighbor or nearest-neighbor position in the equatorial plane, respectively. In addition, the perturbing cation vacancy is determined to be an isolated vacancy, free from any nearby divalent cation. In AgBr, however, no corresponding EPR effects due to the interaction between the hole and the cation vacancy have been observed.

I. INTRODUCTION

In the silver halides, a cation vacancy effectively bears a negative charge and should attract a positive hole in the valence band, thus forming a localized trapped-hole center. The trapping of photocarriers by lattice defects in AgCl and AgBr is of concern, of course, in the attempt to understand the mechanisms of the photographic process. In addition, the trapping of photoholes at cation vacancies in the silver halides is of theoretical interest because of the peculiar electronic composition of the valence band.

Such hole trapping was suggested earlier by Cordone *et al.*[1,2] who interpreted a long-lived photoconductivity in Cd^{2+}-doped silver halides as due to suppression of electron-hole recombination by vacancies introduced by the divalent dopant. Later, Eachus, Graves, and Olm performed electron-paramagnetic-resonance (EPR) studies on irradiated AgCl:Cd^{2+} and found, in addition to the intense spectrum of the normal self-trapped hole (STH), a signal attributed to free electrons.[3] Again, it was proposed that electron-hole recombination was inhibited by hole trapping at cation vacancies. No EPR spectrum from a vacancy-hole center, however, was reported, so that no information was available about its structure or stability.

Further evidence for hole localization at cation vacancies was provided by the optical measurements of Kanzaki and Sakuragi on Cd^{2+}-doped AgCl and AgBr.[4-6] Using novel and sensitive techniques, they showed that band-gap photoexcitation induced a small transient absorption spectrum consisting of a single broad line, in both AgCl and AgBr. This was attributed to a self-trapped hole perturbed by a neighboring cation vacancy; this center persists to temperatures well above 50 K, at which the normal, unperturbed STH in AgCl rapidly disappears.

One expects that a hole-vacancy complex should be paramagnetic.[7] Thus, the present EPR experiments sought to establish the existence, structures, and stabilities of such centers. In order to preclude the electron-hole recombination that would occur upon band-to-band excitation, the holes were produced by sub-band-gap optical ionization of several parts per million (ppm) of Fe^{3+} (or, in some crystals, Cu^{2+}). An excess of cation vacancies was supplied by a second dopant, usually Cd^{2+}, which has a high solubility in the silver halides and is present only in the divalent d^{10} state. As a check that no holes were being trapped by the positively charged dopant itself, the Cd^{2+} was replaced in some crystals by Zn^{2+} or Ca^{2+}. This latter ion has no d electrons at all; hence a comparison of the spectra obtained with different dopants makes a distinction possible between the roles of the dopant itself and the vacancies introduced by it.

In the faced-centered cubic structure of the silver halides, perhaps the most straightforward model for hole trapping at a cation vacancy is one in which the positive hole resides on one or more of the neighboring halide ions, as in the alkali halides. For such a center, the EPR spectrum should reveal the super-hyperfine interactions with the surrounding ions, but with no contribution from the absent Ag^{+}. This is in contrast to the model suggested by Kanzaki and Sakuragi, in which the hole is self-trapped on a nearby silver ion.[8] Now, in the absence of perturbing defects, it is known that at low temperatures the hole is intrinsically self-trapped on a positive silver ion in AgCl,[9] although such a center is only metastable, at best, in AgBr.[10] This localization at a cation is the result of the mixing of the silver d states and the halide p states at the top of the valence band. The resulting self-trapped hole (STH) is essentially a Ag^{2+} center with a Jahn-Teller elongation along a [100] axis of the crystal lattice.[9] Sakuragi and Kanzaki's model for hole trapping at the cation vacancy is thus equivalent to a STH center which is perturbed and stabilized by a neighboring cation vacancy. The position of the perturbing cation vacancy relative to the Ag^{2+} center could, in principle, be either axial or equatorial, and in either a nearest-neighbor or

 ©1990 The American Physical Society

next-nearest-neighbor position. An EPR study should be capable of providing such structural information, details which are not readily accessible from optical and conductivity experiments.

The present paper reports the direct observation of hole trapping at cation vacancies in silver chloride. An analysis of EPR spectra at various temperatures from 20 K to room temperature will be presented to show that in AgCl the stabilized vacancy-perturbed STH model is indeed appropriate for this trapped-hole state. In fact, it will be seen that there exist *two* types of perturbed STH centers, differing in the position of the perturbing cation vacancy, and which are thermally stable to temperatures well above 50 K. The binding energies of the trapped hole to the vacancy will also be estimated from the thermal bleaching temperatures of these new centers. In AgBr, on the other hand, we have seen no corresponding centers, in contrast to the optical results of Sakuragi and Kanzaki.[11]

II. EXPERIMENTAL

Because the silver halides are sensitive to visible light, the experimental procedures were all carried out in the dark or under safe-light conditions. The EPR specimens of silver halides were prepared from large single crystals provided by C. B. Childs of this department. The specimens were oriented by x-ray diffraction and then cut, polished, and etched to the final dimensions of about 3 mm$\times$3 mm$\times$15 mm, with the long axis along a [110] direction.

To introduce a large concentration of cation vacancies, each crystal was doped with one of the three divalent metals, Cd^{2+}, Zn^{2+}, or Ca^{2+}, either by addition to the melt during growth or by solid-state diffusion after crystal growth. The nominal concentrations of these dopants ranged from 50 to 200 ppm. In addition, a second dopant was introduced to serve as a hole source under sub-band-gap irradiation. In one specimen this hole source was copper, but in all of the remaining crystals, iron was added for this purpose.[12] Iron was preferred over copper because it produces fewer EPR lines that interfere with the trapped-hole spectra. Annealing the crystal in a halogen atmosphere at temperatures somewhat below the melting point converted a substantial fraction of the hole-source dopant to its higher-valent state; e.g., from Fe^{2+} to Fe^{3+}. The Fe^{3+} exists in a tetrahedral complex with tightly bound vacancies,[13] and does not introduce any free vacancies into the crystal, in contrast to Cd^{2+}, etc. After rapid cooling from the high-temperature anneal, each specimen was stored at liquid-nitrogen temperature, to prevent aggregation of the dopants.

In the subsequent EPR experiments, irradiation with blue-green sub-band-gap light released holes from Fe^{3+} ions. The resulting Fe^{2+} is essentially invisible to EPR. One advantage of this hole-source method over conventional band-gap excitation is that any new resonance signals appearing after irradiation can thus be safely attributed to trapped-hole centers. Moreover, due to the decrease upon irradiation in the magnitude of signals from the hole-source dopant, the new EPR lines are more readily observed.

In order to reproduce the properties of the well-understood intrinsic self-trapped hole and also to verify the dependence of the new high-temperature STH centers on the presence of an excess concentration of cation vacancies, one specimen was doped only with Fe^{3+}, as the hole source, without addition of any other dopant. This specimen will be referred to as the single-doped specimen, in contrast to the usual double-doped specimens.

The EPR runs were performed on a Brucker ER200tt spectrometer, interfaced to an IBM-compatible personal computer through a Tecmar analog-to-digital (A/D) converter. Both hard-copy and digitized versions of the EPR spectra were generated simultaneously, for later data manipulation and analysis. The temperature of the EPR specimens could be maintained at any value from 5 K to room temperature, and was controlled and measured by Oxford Instruments gas-flow cryogenic equipment.

Sub-band-gap light was provided by a 50-W xenon lamp, transmitted through a blue-UV transmitting extended light pipe, and filtered through a pair of Oriel filters. For the experiments on AgCl, an Oriel band-pass blue filter (BP44, 350 nm $< \lambda <$ 550 nm) was used, together with an Oriel 1% ir-blocking filter (transmission range 280 to 1000 nm) to restrict the irradiation energy to the desired sub-band-gap range. The ir-blocking filter was used to minimize optical bleaching of the trapped hole centers.[14] For experiments on AgBr, the BP44 filter was replaced by an Oriel BP52 green band-pass filter (400 nm $< \lambda <$ 650 nm) in order to allow a deeper penetration into the crystal by the light of longer wavelength. The duration of irradiation at low temperatures was typically in the range of 10 min to more than 1 h; this was usually sufficient to produce saturation in the concentrations of the photoinduced trapped-hole centers.

The thermal behavior and interconversion of the paramagnetic centers was studied by means of a series of isochronal-annealing experiments. The unirradiated crystal was first quenched from room temperature to 20 K, and then irradiated with sub-band-gap light to release holes from the Fe^{3+} ions. The irradiation was followed by a series of 10-min anneals at successively higher temperatures. After each anneal, the EPR spectrum was recorded at 20 K; thus, all analyses and comparisons of EPR spectra were based on spectra taken at the same reference temperature. It will be seen below that the centers remaining above 50 K, at which temperature the intrinsic STH rapidly disappears, have EPR spectra which are only slightly different from that of the intrinsic STH. Thus, the great virtue of the isochronal annealing technique is that steps in the plot of spectral intensity versus annealing temperature give clear indications of changes in the nature of the remaining centers. Such transitions would otherwise be difficult to establish when the shapes of the spectra are similar.

Thermally induced changes in concentration of centers were monitored by the peak heights of two particular lines, chosen because of freedom from interference from the background of other EPR signals. These lines are the high-field $g_{\parallel}$ (denoted by $g_{\parallel}^{R}$) and the third $g_{\perp}$ (denoted by $g_{\perp}^{3}$) lines, as shown in Figs. 1 and 3. As expected, other lines were found to show the same behavior upon iso-

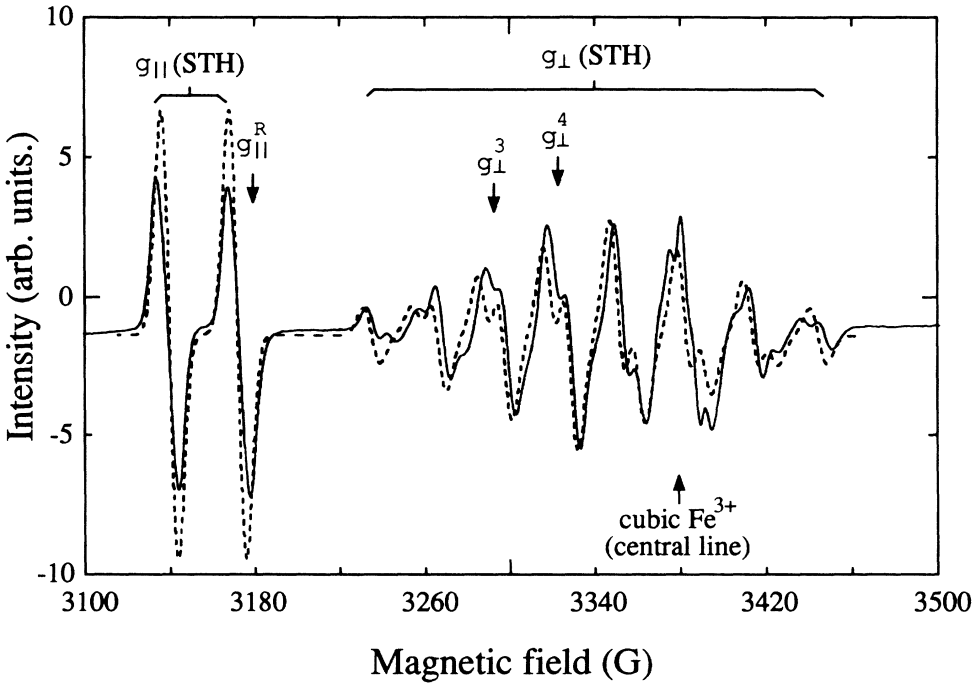

FIG. 1. EPR spectrum, for H||[100], of the intrinsic STH center in AgCl (microwave frequency $\nu=9.45$ GHz); recorded at 20 K during irradiation. The notation $g_{||}^{R}$ denotes the high field line of the $g_{||}$ spectrum; $g_{\perp}^{i}$ refers to the ith line (counting from the left) of the $g_{\perp}$ spectrum. The dashed curve shows a computer simulation.

chronal annealing, but for many of them the measurement of intensities was not as quantitative.

III. EPR RESULTS AND ANALYSIS

A. The intrinsic STH spectrum in AgCl

All of the doped AgCl crystals, upon irradiation at 20 K with sub-band-gap light, showed an intense intrinsic STH spectrum, as well as the expected marked decrease in the intensity of the preirradiation spectrum of Fe^{3+} or Cu^{2+}. The STH spectrum for H||[100], measured at 20 K, is shown as the solid curve in Fig. 1. It is independent of the type and concentration of dopant, and hence is intrinsic. It also agrees in detail with that first reported by Höhne and Stasiw.[9]

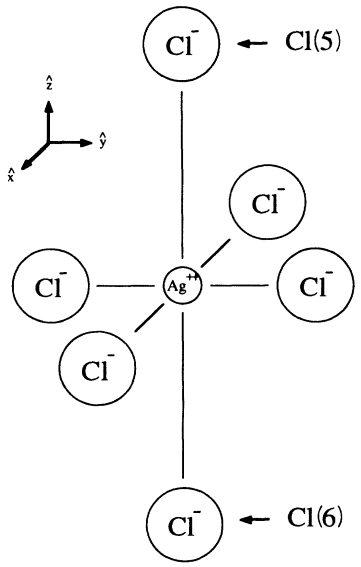

FIG. 2. Structure of the intrinsic STH in AgCl (schematic). The Jahn-Teller elongation is along a [100] axis.

The structure of the axially symmetrical STH is schematically illustrated in Fig. 2. Its EPR spectrum can be well described by the spin Hamiltonian

$$\begin{aligned}\mathcal{H}=&g_{||}\beta H_z S_z+g_{\perp}\beta(H_x S_x+H_y S_y)\\&+A_{||}I_z S_z+A_{\perp}(I_x S_x+I_y S_y)\\&+A(I_z^1+I_z^2+I_z^3+I_z^4)S_z\\&+B[(I_x^1+I_x^2)S_x+(I_y^3+I_y^4)S_y]\\&+B'[(I_x^3+I_x^4)S_x+(I_y^1+I_y^2)S_y]\end{aligned}$$

with the interaction parameter values given by Höhne and Stasiw as follows:

g values: $g_{||}=2.165$, $g_{\perp}=2.041$;

Ag hyperfine: $A_{||}=35$ G, $A_{\perp}=23$ G ;

Cl superhyperfine: $A=0$, $B'=0$;

$$B=\begin{cases}32\text{ G} & \text{for } {}^{35}\text{Cl}\\ 27\text{ G} & \text{for } {}^{37}\text{Cl}\ .\end{cases}$$

This spin Hamiltonian will be employed below in our computer simulation of the spectrum of the vacancy-

stabilized STH center. With this in mind, it is now useful to discuss quantitatively the main features of the STH spectrum.

Because of the difference in the g values with respect to the direction of the magnetic field, the STH spectrum for $\mathbf{H}\|[100]$ consists of two parts, the $g_{\|}$ and $g_{\perp}$ subspectra. The detailed structure of each subspectrum is the result of hyperfine interactions with the central silver ion and superhyperfine interactions with the surrounding chloride ions. Because the interaction parameter for the chloride ions on the symmetry axis [Cl(5) and Cl(6) in Fig. 2] has a vanishing value, it does not appear in the spin Hamiltonian. This indicates that the trapped hole strongly interacts only with the four equatorial Cl ions, as is expected from the Jahn-Teller axial elongation. Moreover, because the perpendicular Cl superhyperfine parameter B' is also zero, only the two equivalent equatorial Cl ions on the axis parallel to the magnetic field $\mathbf{H}$ make contributions to the hyperfine structure for $\mathbf{H}\|[100]$. Therefore, the chloride superhyperfine interactions have almost no effect on the $g_{\|}$ subspectrum, and only two intense EPR lines due to the silver hyperfine interaction are observed in this part of the [100] spectrum. On the other hand, both the silver hyperfine interaction and the chloride superhyperfine interactions contribute to the $g_{\perp}$ subspectrum. If both the Cl isotopes (^{35}Cl and ^{37}Cl) are taken into account, there must exist, in principle, a total of 58 $g_{\perp}$ lines. Due to the fact, however, that the silver hyperfine interaction and the nonzero chloride superhyperfine interactions are approximately equal, the $g_{\perp}$ subspectrum appears to have a nearly symmetrical structure of ony eight resolvable EPR lines, with relative intensities 1:3:5:7:7:5:3:1.

One of the characteristic properties of the STH center is its instability against both thermal annealing and optical bleaching. Thus, either heating above 40 K or irradiation with red light can readily destroy this paramagnetic center. Paul has made a detailed study of the thermally activated decay of the photoproduced STH, and found that above 50 K its lifetime is less than 1 min.[15] In fact, in the isochronal-annealing experiments, this important property is the determining effect that unambiguously reveals the existence of the new paramagnetic centers.

B. Post-anneal spectra: New, more stable centers

Although the STH spectrum recorded after sub-band-gap irradation at 20 K was found to be independent of the type and concentrations of dopants in the AgCl crystals, a subsequent annealing at temperatures above 50 K, at which the intrinsic STH rapidly disappears, resulted in spectra which did indeed depend, in both shape and intensity, on the presence of divalent dopants. For the single-doped specimen (Fe^{3+} only), the post-anneal spectrum (recorded at the reference temperature 20 K) was identical to that before irradiation. Thus, in this specimen, which contained only a negligible amount of free cation vacancies, the STH completely disappeared when the temperature was increased above 50 K, and no new center other than the expected Fe^{3+} was formed.

For all of the double-doped specimens, however, which contained high concentrations of cation vacancies, after a post-irradiation anneal at temperatures above 50 K there remained a somewhat weaker spectrum very similar to,

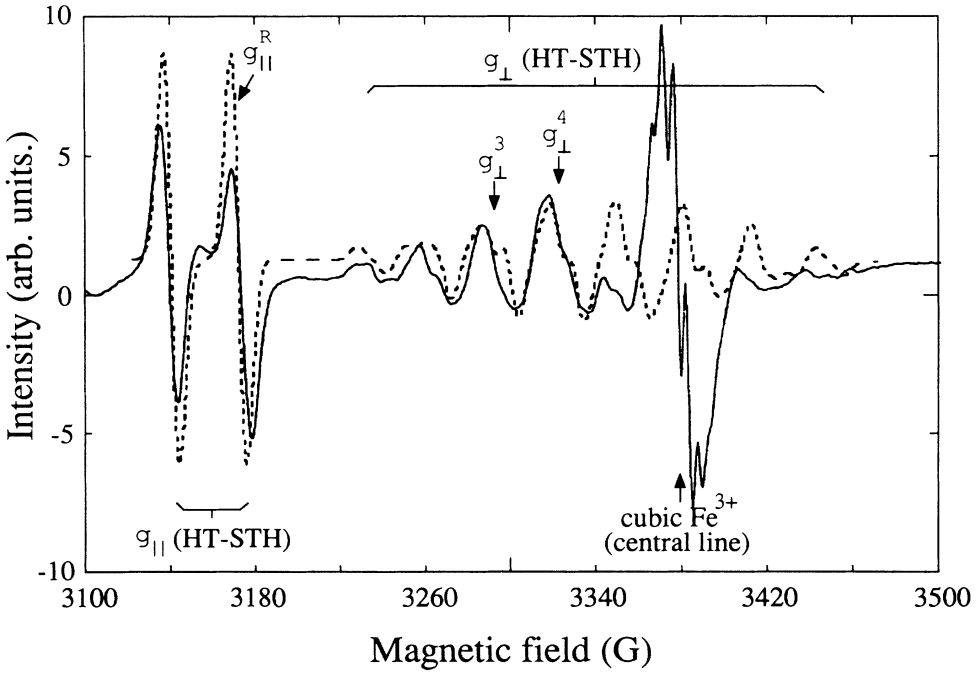

FIG. 3. Measured and simulated EPR spectra, for $\mathbf{H}\|[100]$, of the less stable HT-STH center in AgCl (microwave frequency $\nu=9.45$ GHz). This measured spectrum (solid curve) was recorded at 20 K after 60 K annealing at the end of a 20 K irradiation. The simulated spectrum (dashed curve) was calculated with the superhyperfine parameter value for one of the equatorial Cl ions increased by 15%, as described in Sec. III E.

but not identical to, the original STH spectrum. This new spectrum was embedded in the partially restored cubic Fe^{3+} spectrum. Due to its similarly to the intrinsic STH spectrum and its persistence to temperatures well above 50 K, this STH-like signal will be referred to as the high-temperature STH (HT-STH) spectrum.

The solid curve in Fig. 3 shows the high-temperature STH spectrum of a double-doped crystal containing 132 ppm Cd^{2+}, recorded at 20 K after an anneal at 60 K for 10 min, following irradiation at 20 K. An identical spectrum (except for overall intensity) was also obtained for each of the other double-doped specimens, independent of the type and concentration of the divalent cation (Ca^{2+}, Cd^{2+}, or Zn^{2+}) and also independent of the ion added to serve as the source of holes (e.g., Fe^{3+} or Cu^{2+}). In gross appearance, this high-temperature STH spectrum shows no obvious difference from the normal STH spectrum, but there are several significant quantitative changes. For example, the $g_\perp$ lines are not as sharply featured as were the eight strong $g_\perp$ lines of the intrinsic STH spectrum and they are now noticeably weaker, relative to those of the $g_\parallel$ subspectrum. This change in relative intensities suggests that the two interacting equatorial chloride ions of the STH center are no longer equivalent. This, in turn, implies that in the new centers there are small deviations from the axially symmetrical structure of the intrinsic STH. In other words, the HT-STH centers must be stabilized and perturbed by some defect(s) near to the equatorial chloride ions.

The high thermal stability of the new spectrum and the change in the ratio of line intensities demonstrate that we are dealing with distinctly different defects, although with a structure closely related to that of the STH. The existence of these new HT-STH centers will be clearly shown in the isochronal-annealing results, discussed in the following section. In addition, the fact that the shape of the post-anneal spectrum in the double-doped specimens is independent of the type of divalent dopant indicates that the new centers do not involve the dopant ions themselves. Furthermore, the absence of this new spectrum in the single-doped specimen, which contains very few cation vacancies, implies that the formation of the HT-STH centers requires the presence of excess cation vacancies. One thus concludes that the high-temperature STH centers are simply self-trapped holes which have migrated to and become stabilized (and perturbed) by a nearby cation vacancy.

The HT-STH spectrum can also be produced in the double-doped specimens by irradiation at temperatures well above 50 K, where the intrinsic STH becomes very mobile. Thus, the "perturbed" STH center can also be produced by the trapping of a *free* positive hole at a negative cation vacancy, perhaps transiently passing through the STH state. The higher thermal stability of the new centers is presumably the consequence of the electrostatic and elastic interaction between the negatively charged cation vacancy and the positively charged, axially distorted STH.

As a matter of fact, the HT-STH centers may have earlier been observed by Zhitnikov, Lipatov, and Romanov,[16] who reported an EPR spectrum which they attributed to the STH, but which was stable up to about 120 K, in AgCl crystals of only moderate purity (and therefore containing substantial concentrations of vacancies). In addition, Stulen and Ascarelli[17] observed two components in the temperature dependence of the luminescence from self-trapped excitons. One of these was stable only at temperatures below 40 K, and the other survived to much higher temperatures. Consistent with our present results, they suggested that the second component was due to a self-trapped exciton near a defect, presumably a cation vacancy.

C. Isochronal annealing experiments: Effect of vacancies

In order to unambiguously demonstrate the presence of the new HT-STH centers in the double-doped AgCl specimens, isochronal-annealing experiments, as described in Sec. II, were performed. Figures 4 and 5 show typical results on the single-doped and a double-doped specimen, respectively. In each figure, the intensities of the selected $g_\parallel^R$ and $g_\perp^3$ lines of the post-anneal spectra, each normalized to the original intensities of their counterparts in the intrinsic STH spectrum, are plotted as functions of the annealing temperature. These normalized intensities serve as a measure of the surviving STH populations, both "intrinsic" and "high temperature," after annealing at successively higher temperatures.

As indicated in Fig. 4, the STH in the single-doped specimen starts to decay substantially at 35 K and has completely disappeared after the anneal at 40 K. This is just as expected for the intrinsic STH.[4,15] Also, as expected, both the $g_\parallel^R$ and $g_\perp^3$ lines behave in the same way in this specimen: they decay identically, as indicated by the complete overlap of the two curves. Thus, in the absence of deliberately added excess vacancies, the irradiated crystal contains only one type of hole center, the "intrinsic" STH center.

For the double-doped specimens, however, with their large concentrations of cation vacancies, Fig. 5 shows

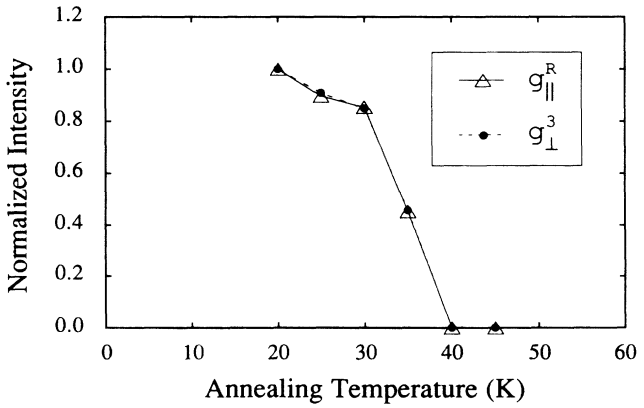

FIG. 4. Intensities of selected lines, normalized to their original 20 K values, as a function of annealing temperature, for the single-doped specimen. The specimen was doped with 19 ppm Fe^{3+} as a source of holes; it contained no other deliberately added cations.

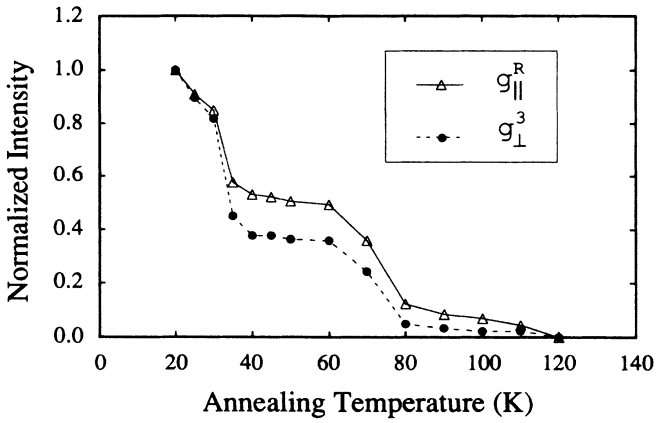

FIG. 5. Plot of isochronal annealing data as in Fig. 4, but now for a double-doped specimen. The specimen was doped with 20 ppm Fe^{3+} as a source of holes and 132 ppm Cd^{2+} to introduce an excess of cation vacancies.

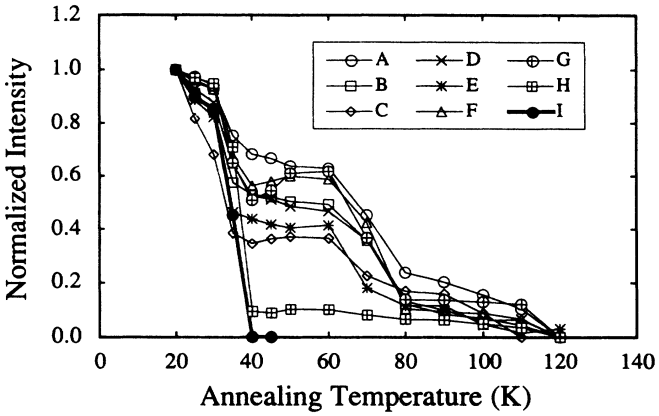

FIG. 6. Plot of isochronal data for the $g_{\parallel}^{R}$ line for all of the specimens. The heavy solid curve represents the data of the single-doped specimen, which did not contain excess cation vacancies. Double-doped specimens: *A*, 209 ppm Cd; *B*, 132 ppm Cd; *C*, 50 ppm Cd; *D*, 50 ppm Cd; *E*, 50 ppm Cd; *F*, 80 ppm Ca; *G*, 80 ppm Ca; *H*, 63 ppm Zn. Single-doped specimen: *I*, 19 ppm Fe only.

that the behavior is more complex and that the decay curves for the two spectrum lines do not coincide. The most striking feature is the survival of a substantial signal after annealing at 40 K, due to vacancy stabilized centers, the concentration of which stays approximately constant until about 60 K. Then, above 80 K, there appears another nearly flat region of a roughly constant population. The EPR intensity vanishes completely only after annealing at 120 K, a temperature which is about three times higher than the bleaching temperature of the intrinsic, unperturbed STH center. Also, although the step temperatures in Fig. 5 are the same for both of the lines monitored, the magnitudes of the drops differ, showing that the EPR spectrum changes shape at each step. These two observations—the two steps and the changes in spectrum shape—indicate that there are actually two types of high-temperature center, one of which is stable to about 70–80 K and the other to about 110–120 K.

In order to further document the presence of the two new centers, the results of the entire set of isochronal experiments on all nine of our specimens, including both single- and double-doped, are summarized in Fig. 6 for the $g_{\parallel}^{R}$ line; similar results were also obtained for the $g_{\perp}^{3}$ line. One sees that the temperature ranges of the plateaus and the steps are the same for all double-doped specimens. Thus, the first flat region and the first drop must correspond to the population and the fast decay of the normal, intrinsic STH, while the other two sets of plateaus and steps demonstrate the existence of the two new centers.

That the shape, as well as the intensity, of the spectrum changes upon annealing above 35 K is quantitatively demonstrated by considering, for example, the ratio of intensities of the $g_{\parallel}^{R}$ and $g_{\perp}^{3}$ lines. At the 35 K drop the $g_{\perp}^{3}/g_{\parallel}^{R}$ intensity ratio was found to fall by 20% to 45% for the various crystals studied; it then remained constant across the entire 40–70 K plateau. Thus, the spectrum observed in this plateau must be due to a new center. Because of the similarity of its EPR spectrum to that of the intrinsic STH, however, and because its existence requires the presence of a large concentration of cation vacancies, this new center (HT-STH) must be a complex of a STH with a nearby charge-compensating cation vacancy. The decrease in the $g_{\perp}^{3}/g_{\parallel}^{R}$ intensity ratio can then be understood in terms of the broadening of the $g_{\perp}$ lines, caused by perturbation by the vacancy.

A similar analysis of shape change cannot be made for the other, more stable HT-STH center, the one that persists above the second drop at 70 K. Because of the low intensity of its signal, together with an increase in the background Fe^{3+} signals, there is now a much greater experimental error in the measurement of line intensities. It is clear, nevertheless, from the drop at 70 K to a lower plateau that there are, indeed, two distinctly different HT-STH centers, readily distinguished by their thermal stabilities. This conclusion illustrates the utility of the isochronal annealing technique is providing information that could not be obtained simply from analysis of the EPR spectrum.

It had earlier been found that in AgCl the binding energy of a cation vacancy to a neighboring divalent cation is close to 0.25 eV, almost independent of whether the vacancy is in the nearest-neighbor or the next-nearest-neighbor position.[18–20] If a similar approximate equality applies to the energies of complexes of a cation vacancy with a STH (which has the same effective charge as does a divalent cation), then it seems reasonable that the two vacancy-stabilized centers revealed by the isochronal experiments are defects in which the vacancy is in a nearest-neighbor or next-nearest-neighbor position, relative to the Ag^{2+} ion of the STH. Further detailed evidence supporting this is presented below.

D. The nature of the perturbing cation vacancy

Having demonstrated, from isochronal-annealing runs, the existence of two new HT-STH centers, identified as vacancy-STH complexes, two immediate structural questions arise: (a) Is the cation vacancy free or also bound to a divalent cation? (b) For each of the two HT-STH defects, where is this cation vacancy located, relative to the axis and center of the STH? The second question is equivalent to asking how the thermal stability of the HT-STH centers depends on the position of the binding vacancy.

As to the nature of the perturbing vacancy (free or impurity associated), one notes that Fig. 6 shows that the HT-STH population is exceptionally low in the case of the Zn^{2+}-doped specimen, for which the binding energy of the impurity-vacancy complex is known to be unusually high.[21] This suggests that the vacancy involved in the HT-STH center is the free vacancy, as would be expected from electrostatic considerations, and not the impurity-vacancy complex. This is further corroborated by the observation that the shape of the spectrum of the HT-STH is the same for all divalent dopants employed. Finally, it is also consistent with the observation of Abraham *et al.*[22] that in MgO, holes trapped at isolated cation vacancies are much more stable than those trapped at the partially compensated impurity-vacancy complexes.

The proposal that the vacancy in the HT-STH is not associated with a divalent cation was confirmed by measurement of the effect of the concentration of Cd^{2+} on the resulting population of HT-STH centers. In Fig. 7, the HT-STH concentration at 60 K, as monitored by the intensities of the $g_{\parallel}^{R}$ and the $g_{\perp}^{3}$ lines, is plotted against the nominal cadmium concentration. The mass-action law, which governs the vacancy-impurity association equilibrium, shows that a plot of the concentration of impurity-vacancy complexes versus total dopant content must have a positive curvature, while that for the free vacancy has a negative curvature. The negative curvature of the plots of Fig. 7 shows clearly that it is the free cation vacancy that participates in the HT-STH centers.

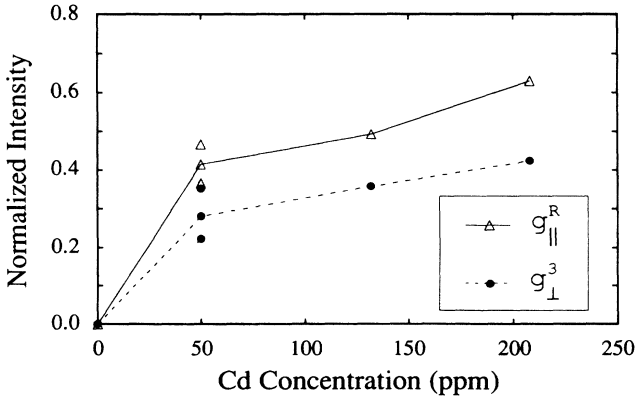

FIG. 7. Dependence of the HT-STH population on the Cd^{2+} concentration. The curves are drawn simply by connecting the data points, in order to show the trend.

E. The position of the silver vacancy

One now asks where, relative to the axially symmetric STH structure, is this vacancy located? The close similarity in appearance of the HT-STH spectrum to that of the intrinsic STH not only obscured the identification of the HT-STH centers by previous researchers,[16] but also now makes difficult the task of locating the position of the perturbing vacancy. To answer this question, one must consider the effects on both the $g_{\parallel}$ and $g_{\perp}$ subspectra due to the vacancy at various positions.

Four possible configurations for the cation vacancy-trapped hole complex are illustrated in Fig. 8. In each of these models, the vacancy resides at either a nearest-neighbor or a next-nearest-neighbor position. For a cation vacancy beyond these two closest cation shells, it is presumed that there would be no significant interaction with the trapped hole.

Since the spatial distribution of the trapped hole in the STH center is characterized by the ground state $|x^2-y^2\rangle$ of the silver d^9 configuration, it interacts strongly only with the four neighboring chloride ions on the equatorial plane.[9] For example, no chloride superhyperfine structure from the axial Cl(5) and Cl(6) is resolved in the $g_{\parallel}$ region of the [100] spectrum (Fig. 1). Then, because the vacancy of model 1 is even farther away than are the axial anions, it would not significantly perturb the STH; one can thus exclude this as the structure of either of the two HT-STH centers. Moreover, the small but measurable change in the $g_{\perp}$ line shape after annealing above 50 K, as well as the change in the ratio of intensities of the $g_{\perp}$ and $g_{\parallel}$ subspectra, have already been shown to imply the existence of a cation vacancy adjacent to the equatorial chloride ions. All of the remaining three models of Fig. 8 fulfill this requirement. Of these, however, model 2 can

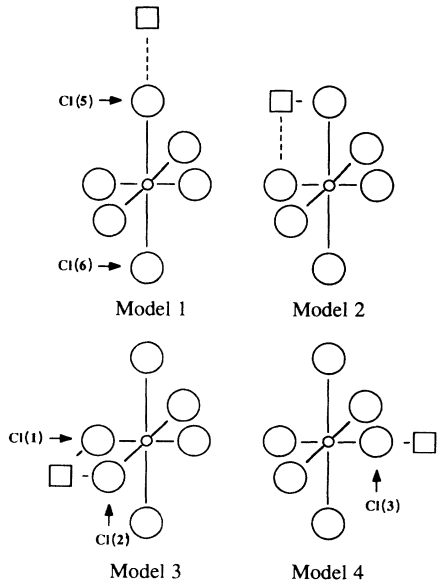

FIG. 8. Possible models for the HT-STH centers. The small circle in the center of each model represents the Ag^{2+} ion, the square represents the vacancy.

be ruled out because the proximity of the vacancy to the axis is inconsistent with the observed axial symmetry of the HT-STH spectra.

In the remaining possibilities, models 3 and 4, the vacancy is somewhat further from the symmetry axis and also the horizontal reflection plane is preserved. In addition, the proximity of the vacancy to one or two of the equatorial chlorides is consistent with the changes in the spectrum that result upon conversion of the intrinsic STH to the HT-STH centers. If these two models really do represent the two different centers that are revealed by the isochronal annealing plots, then the difference in their thermal stabilities would naturally follow from the different locations of the charge-compensating cation vacancy.[23]

In order to investigate this proposal, a computer program was developed to simulate the EPR spectra of the various possible structures of the peturbed STH centers. As a check on the validity of the simulation, and using the interaction parameter values given by Höhne and Stasiw (and confirmed in our experiments),[9] the simulation program was found to reproduce the known intrinsic STH spectrum very well, as shown by the dashed curve in Fig. 1. Figure 1 also shows that there are two minor discrepancies with the measured spectrum: (i) a small deviation in the shape of the outer lines of the $g_\perp$ subspectrum, which is due to the fact that the simulation does not take into account the presence of a second chlorine isotope and (ii) the ratio of intensities of the $g_\perp$ lines to those of the $g_\parallel$ lines is about 20% too small, presumably a result of the simplifying assumption that both of the subspectra have the same line shape.

This program was then employed to simulate the EPR spectra to be expected from models 3 and 4 of Fig. 8. The goal, of course, is to compare the observed HT-STH spectra with the simulated ones, in order to make assignments. In practice, the signal remaining after the 70 K anneal, which destroyed the less stable HT-STH, was found to be too weak to permit of a definitive comparison. Thus, we sought to use the simulation only to identify the less stable HT-STH center, i.e., the center responsible for the spectrum observed at the 40–70 K plateau. The other, more stable center is then to be identified by elimination between models 3 and 4.

In the calculation, it was assumed that the cation vacancy perturbs only near-neighbor chloride ions, numbers 1, 2, and 3 of Fig. 8. The resulting relaxation of these ions will change the value of the chloride superhyperfine parameter; hence this was treated as a fitting parameter. Because of the discrepancies mentioned above, especially that due to the line-shape simplification, a direct fitting of the measured spectrum to get the interaction parameter values in the spin Hamiltonian is not possible. Instead, comparisons were made between the observed and simulated intensity ratios $g_\perp^3/g_\parallel^R$ (as the basic criterion of the fit) and $g_\perp^3/g_\perp^4$ (as a measure of the overall shape of the $g_\perp$ subspectrum), where $g_\perp^4$ is the fourth $g_\perp$ line from the low-field side as shown in Figs. 1 and 3. These ratios are again normalized to their counterparts calculated from the measured and simulated intrinsic STH spectra.

It proved to be impossible to obtain a fit of the experimental spectrum of the less stable HT-STH center on the basis of he nearest-neighbor configuration of model 3. For example, values of the chloride superhyperfine parameter that approximately reproduced the experimental normalized $g_\perp^3/g_\parallel^R$ intensity ratio, gave a simulated normalized $g_\perp^3/g_\perp^4$ ratio that was too high by an unacceptable 25%.

For the center of model 4, however, a satisfactory fit could indeed be obtained. While the small inaccuracies of the simulation program and the unavoidable background in the experimental spectrum made impractical the direct fitting of the entire measured spectrum, as seen in Fig. 3, nevertheless the observed normalized $g_\perp^3/g_\parallel^R$ and $g_\perp^3/g_\perp^4$ ratios, could be well reproduced (within about 10%) upon judicious choice of the chloride superhyperfine parameter. As seen in Fig. 3, the simulated spectrum showed no background interference and also a more resolved $g_\perp$ subspectrum, presumably because of the neglect of the ^{37}Cl isotope. Otherwise, it reproduced the measured spectrum reasonably well. Thus, one can confidently conclude that the less stable HT-STH center is the next-nearest-neighbor complex of model 4. Presumably, then, the more stable HT-STH, the center that is seen in the range 80–110 K, must be the nearest-neighbor complex of model 3. This assignment is certainly consistent with electrostatic expectations of the relative stabilities.

In fact, there were two different values of the chloride superhyperfine parameter which produced a satisfactory fitting of model 4 to the less stable HT-STH spectrum: 0.80 and 1.15 times the value for the intrinsic STH. The smaller value would correspond to a vacancy-induced relaxation of the equatorial Cl(3) ion away from the central Ag^{2+}; the larger value corresponds to an inward relaxation. It now remains to determine which of the two values is most suitable. This is equivalent to asking whether the Cl(3) ion moves inwards to or outwards from the central Ag^{2+} ion as a result of the presence of the cation vacancy. This question cannot be answered from the EPR data, but guidance can be sought from prior studies of the pressure dependence of ionic conductivity in alkali and silver halides.[24–26] For the silver halides, unfortunately, one cannot deduce the sign of relaxation about the vacancy, because its formation volume is coupled with that of an interstitial. In the case of the alkali halides, however, the formation volume of Schottky pairs was found to be greater than the molecular volume, indicating a relaxation of nearest ions away from the vacancies. If this is also true for the cation vacancy in the silver halides, then it would result in a displacement of the Cl(3) ion toward the Ag^{2+}, increasing the superhyperfine interaction above that of the intrinsic STH. Moreover, since the symmetry of this HT-STH center is not observed to deviate significantly from axial, the distortion on the equatorial plane must be small enough that the structure of the center is not dramatically changed. From these two considerations, it thus appears that the next-nearest-neighbor model, with a small increase (15%) in the superhyperfine interaction, quite satisfactorily accounts for the spectrum of the less stable HT-STH center.

One notes that a silver site which is a next-nearest neighbor to the vacancy (i.e., the configuration of model 4) is likely to be the first which a migrating photohole would encounter, en route to becoming trapped to form a perturbed HT-STH center. If this center were more stable than that with the nearest-neighbor configuration (model 3), then it is unlikely that the latter would ever be formed. Thus, the fact that there are three steps in the isochronal-annealing curves, rather than only two, further supports the assignments which we have made for the two HT-STH centers.

As a further check, Kopelman has carried out additional experiments, but this time using band-to-band excitation and the conventional electron-trap method to minimize electron-hole recombination.[27] The AgCl specimens were doped with Cd^{2+} or Ca^{2+} to enhance the concentration of cation vacancies, and also with Pd^{2+}, which functions as an electron trap. The observed effects on the EPR spectra of isochronal annealing of these crystals reveal a behavior which is identical to that described above. Thus, the conclusions reached in this section about the nature of the HT-STH centers in AgCl are confirmed to be independent of the detailed nature of both the dopants and the method of photocarrier excitation.

F. EPR results in AgBr

Similar experiments have also been made on AgBr crystals doped and prepared in the same way as the AgCl specimens. In every case, no resonance other than the well-known spectrum[28] of cubic Fe^{3+} was seen. The only effect of irradiation (both band-gap and sub-band-gap) was to reduce the intensity of this spectrum, presumably because some photoholes had become trapped at other sites that are invisible to EPR, such as crystal dislocations, with their large strain fields.

IV. DISCUSSION

A hole trapped at a cation vacancy has been called "the antimorph of the F center."[29] In alkali halides, such a paramagnetic center, the V_F center, is known to be a hole shared by two adjacent halide ions near a cation vacancy. Thus, the V_F center is essentially a self-trapped hole (the V_K center) stabilized by an adjacent cation vacancy.[30] The hole centers which we have found in AgCl are also vacancy-perturbed self-trapped holes, although in this case the mixing of states at the top of the valence band results in a STH centered on a single cation, in contrast to the two-halide-centered STH of the alkali halides. One result of this difference is that in AgCl the vacancy is further removed from the hole, so that the EPR spectrum of the HT-STH much more closely resembles that of the intrinsic STH than is observed in the alkali halides. It is for this reason that the technique of isochronal annealing was so useful in revealing the presence of new centers which had been previously overlooked in conventional EPR experiments on AgCl.

Two other centers, each involving an impurity ion in silver chloride, but with geometries similar to those of the HT-STH centers, have been reported. The photographically important Rh^{2+} dopant in AgCl has been found to form a [100] axial center.[31] Here, too, a stabilizing cation vacancy is located at a next-nearest-neighbor site in the equatorial plane, and, as in the case of our HT-STH center, the apparent axial symmetry of the $(RhCl_6)^{4-}$ is preserved. Similarly, a STH has been found to be stabilized by a single bromide impurity ion located at a nearest-neighbor site in the equatorial plane.[32,33] Here, however, the closer proximity of the perturbing ion produces a pronounced deviation from axial symmetry of the EPR spectrum.

The depth of traps for photocarriers is a parameter of great interest; this is especially true in this case, with its photographic implications. Unfortunately, whereas optical transition energies are in some cases available, thermal trap depths are rarely known, and thus even semiquantitative estimates are of considerable value. One can obtain such estimates for the two HT-STH centers of the present work from a comparison of their thermal bleaching temperatures with that of the intrinsic STH, which has a migration energy of 0.062 eV and appears to have a thermal trap depth of about 0.12 eV.[34,35] Taking ratios of the bleaching temperatures (which is equivalent to ignoring differences in the preexponential factors), and comparing with the migration energy of the STH, one estimates the energies to separate the bound STH from its stabilizing vacancy to be approximately 0.12 and 0.19 eV for the next-nearest-neighbor and the nearest-neighbor centers, respectively. Then, adding on the 0.12 eV depth of the STH potential well, one obtains about 0.24 and 0.31 eV for the thermal ionization energy of the hole in the two HT-STH centers. Interestingly, these values are comparable to the estimate of the binding energy of a hole-vacancy complex in AgBr, 0.30 eV, obtained by Burberry and Marchetti[36] from optically detected magnetic-resonance experiments; unfortunately, equivalent results are not available for AgCl. We have no explanation of why our EPR experiment did not reveal such centers in AgBr, except to point out that the intrinsic STH is unstable in AgBr;[37] thus, even with stabilization by a vacancy, the lifetime of the corresponding HT-STH may be too short for ready observation by EPR.

V. CONCLUSIONS

From a detailed study of the isochronal annealing of the EPR spectra in variously doped AgCl crystals, the present work has identified the centers formed by the trapping of a photohole at a cation vacancy. There exist two types of high-temperature self-trapped hole (HT-STH) centers, which are identified as self-trapped holes stabilized by a nearby cation vacancy. The nature and the position of the perturbing cation vacancy were determined from the dependence of the HT-STH population on the divalent cation concentration and from comparison of computer-simulated spectra with the measured spectrum. It could thus be concluded that, in AgCl, the vacancy that binds the positive hole is not associated with a divalent cation, and that it is located on an equatorial site, at either a next-nearest-neighbor or nearest-neighbor position, with the latter being more stable. The trap depths, relative to the free delocalized hole, are estimated

to be about 0.24 and 0.31 eV for the two centers.

In AgBr, on the other hand, no EPR signal arising from any comparable center has been observed. The instability of the intrinsic STH in AgBr may possibly explain the absence of such a resonance.

ACKNOWLEDGMENTS

We thank C. B. Childs for growing all the crystals used in this work. This research was supported by the National Science Foundation, under Grant No. DMR-8722476.

[1]L. Cordone and M. U. Palma, Phys. Rev. Lett. **16**, 22 (1966).
[2]L. Cordone, S. L. Fornili, S. Micciancio, and M. U. Palma, Phys. Rev. Lett. **188**, 1404 (1969).
[3]R. S. Eachus, R. E. Graves, and M. T. Olm, Phys. Status Solidi B **88**, 705 (1978).
[4]H. Kanzaki and S. Sakuragi, Solid State Commun. **9**, 1667 (1971).
[5]H. Kanzaki and S. Sakuragi, Photogr. Sci. Eng. **17**, 69 (1973).
[6]H. Kanzaki, J. Photogr. Sci. **32**, 117 (1984).
[7]R. S. Eachus and J. P. Spoonhower, Photogr. Sci. Eng. **26**, 20 (1982).
[8]H. Kanzaki, Semicond. Insulators **5**, 517 (1983).
[9]M. Höhne and M. Stasiw, Phys. Status Solidi **28**, 247 (1968).
[10]E. Laredo, W. B. Paul, S. E. Wang, L. G. Rowan, and L. Slifkin, in *The Physics of Latent Image Formation in Silver Halides*, edited by A. Baldereschi, W. Czaja, E. Tosatti, and M. Tosi (World Scientific, Singapore, 1984), p. 35.
[11]H. Kanzaki, Photogr. Sci. Eng. **24**, 219 (1980).
[12]Chien-teh Kao, Ph.D. thesis, University of North Carolina at Chapel Hill, 1989.
[13]W. Hayes, J. Pilbrow, and L. Slifkin, J. Phys. Chem. Solids **25**, 1417 (1964).
[14]L. Cordone, S. L. Fornili, S. Micciancio, and M. U. Palma, Phys. Rev. Lett. **26**, 26 (1971).
[15]W. B. Paul, S. Goldenberg, L. Rowan, and L. Slifkin, Cryst. Latt. Defects Amorph. Mater. **15**, 197 (1987).
[16]R. A. Zhitnikov, V. D. Lipatov, and N. G. Romanov, Fiz. Tverd. Tela (Leningrad) **15**, 929 (1973) [Sov. Phys.—Solid State **15**, 645 (1973)].
[17]R. Stulen and G. Ascarelli, Phys. Rev. B **15**, 1161 (1977).
[18]D. Golopentia and L. Slifkin, Phys. Status Solidi A **72**, 123 (1982).
[19]L. M. Dutta, Ph.D. thesis, University of North Carolina at Chapel Hill, 1975.
[20]R. Lieb, Ph.D. thesis, University of North Carolina at Chapel Hill, 1976.
[21]A. Batra and L. Slifkin, Phys. Status Solidi A **19**, 171 (1973).
[22]M. Abraham, Y. Chen, and W. Unruh, Phys. Rev. B **9**, 1842 (1974).
[23]R. S. Eachus, R. E. Graves, and M. T. Olm, J. Chem. Phys. **69**, 4580 (1978).
[24]I. Hooton and P. W. M. Jacobs, Can. J. Chem. **66**, 830 (1988).
[25]A. E. Abey and C. T. Tomizuka, J. Phys. Chem. Solids **27**, 1149 (1965).
[26]B.-E. Mellander and D. Lazarus, Phys. Rev. B **29**, 2148 (1984).
[27]E. Kopelman, M. S. thesis, University of North Carolina at Chapel Hill (in preparation).
[28]K. Hennig, Phys. Status Solidi **3**, 91 (1963).
[29]F. Seitz, Rev. Mod. Phys. **26**, 7 (1954).
[30]W. Känzig, J. Phys. Chem. Solids **17**, 80 (1960).
[31]M. T. Olm, J. R. Niklas, J. M. Spaeth, and M. C. R. Symons, Phys. Rev. B **38**, 4343 (1988).
[32]M. Yamaga, Y. Hayashi, and H. Yoshioka, J. Phys. Soc. Jpn. **44**, 154 (1978).
[33]M. Yamaga and H. Yoshioka, J. Phys. Soc. Jpn. **46**, 1538 (1979).
[34]N. F. Mott and A. M. Stoneham, J. Phys. C **10**, 3391 (1977).
[35]E. Laredo, W. B. Paul, L. Rowan, and L. Slifkin, Phys. Rev. B **27**, 2470 (1983).
[36]M. S. Burberry and A. P. Marchetti, Phys. Rev. B **32**, 1192 (1985).
[37]A. Sumi and Y. Toyozawa, J. Phys. Soc. Jpn. **35**, 137 (1973).